A study of coupled magnetic fields for an optimum torque generation

Nurulasikin Mohd Suhadis[1,*], Renuganth Varatharajoo[2]
[1]School of Aerospace Engineering, Engineering Campus, Universiti Sains Malaysia, 14300 Nibong Tebal, Pulau Pinang, Malaysia.
[2]Department of Aerospace Engineering, Faculty of Engineering, Universiti Putra Malaysia, 43400 Serdang, Selangor, Malaysia.
[*]E-mail: normatsue@yahoo.com

ABSTRACT

Magnetic torquers are specifically designed to generate a magnetic field onboard the satellites for their attitude control. A control torque is generated when the magnetic fields generated by the magnetic torquers couple with the geomagnetic fields, whereby the vector of the generated torque is perpendicular to both the magnetic fields. In this paper, two control algorithms for a momentum bias satellite implementing two and three magnetic torquers onboard have been developed. The structured algorithms are for an optimum torque generation and eventually controlling the satellite attitudes (roll/yaw) and nutation using a proportional (P) controller as well as managing the excess angular momentum via a proportional-integral (PI) controller. The developed control algorithms were tested using the complex and simplified geomagnetic field models for a LEO satellite mission in a nominal attitude operation. Their attitude torque generation performances were compared and it is found that the optimum torques can be generated by both the developed control algorithms. However, the system with three magnetic torquers provides a better torque generation compartment and consequently gives a better attitude performance up to 0.5 deg.

Keywords: Coupled magnetic fields, magnetic torquer, magnetic attitude control system

1. INTRODUCTION

Satellites are exposed to the presence of natural environmental forces during their lifetime. The interaction between these forces and the satellite will generate several types of dominant disturbance torque which significantly affect the orbital and attitude motions of the satellite. Their magnitudes are a function of the satellite's altitude and design. Without any counterbalance action, the satellite performance will gradually deteriorate and eventually fail the mission. Fortunately, these generated disturbance torques can be manipulated for stabilization and control purposes when they are generated in a desirable amount and direction. The use of these torques for passive and semi passive attitude controls are possible [1]. One of the most significant disturbance torques for small satellites operated in Low Earth Orbit (LEO) is the magnetic torque. It is generated when the magnetic fields generated by the electrical equipments onboard the satellite couples with the geomagnetic fields. The magnetic dipole moment within the satellite can be generated in various ways whether by using permanent magnets, hysteresis rods or current-carrying coils/magnetic torquers [2].

Permanent magnet and hysteresis rod provide unalterable and constant magnetic dipole moment values thus providing a passive means of attitude stabilization. In contrast, the current-carrying coil/magnetic torquer provide an active means of attitude control where they have an ability to generate controllable values of magnetic dipole moment.

The earliest idea of the passively magnetic control technique was to align the single spin stabilized satellite along the direction of the geomagnetic field simply by placing a permanent magnet onboard the satellite. It is because a satellite that has a large magnetic dipole moment onboard acts similar to a simple compass which tends to align itself along the local direction of the geomagnetic field. As reported by Fischell [3], the first magnetically oriented satellite called Transit 1B was launched on 13 April 1960 into a polar orbit. The permanent magnet was placed along its axis of rotation has an average of two revolutions per orbit. This passive technique is suitable for the mission that requires monitoring over one part of the earth hemisphere and has been successfully implemented in several satellites as in Spartnik micro-satellite developed by San Jose State University where the mission was to observe over the northern hemisphere [4]. Munin was developed by Swedish Institute of Space Physics for data collection on the auroral activity on both the northern and southern hemispheres [5]. Unisat-4 was developed by University of Rome for ionospheric plasma monitoring [6]. Onboard these satellites, the magnetic hysteresis rod damper were also used to magnetically damp the excessive spin energy to control the spin rate of the satellite body.

The idea of the active magnetic control technique was probably first reported by White et al. [7]. In their study, the feasibility of obtaining a magnetic torque about all three satellite's axis using 2 or 3 current carrying coils was investigated. It was found that control about all three axes can be obtained in an intermittent basis where only two axes can be controlled simultaneously at one time. This finding led researches to implement this technique on various satellite configurations. Ergin and Wheeler [8] amongst the first implemented this active technique on a spin stabilized satellite. They developed control laws to align the spin axis of a satellite normal to the orbital plane. The required torque, which is normal to the spin axis, was obtained using the current carrying coils placed along the satellite's spin axis. Further, Wheeler [9] developed control law for the nutation damping as well as the position control. These are amongst the earliest researches carried out for an active magnetic attitude control of spin stabilized satellite where later exploited on various missions. SCD-1 [10] and SACI-1 [11] are amongst spin stabilized satellite flown with active magnetic attitude control.

All these earlier findings show that the use of magnetic technique to stabilize and control the satellite has been considered as a very attractive method since the earliest satellites were launched. Many researchers have implemented this technique on a gravity gradient stabilized satellite [12, 13], a momentum bias satellite [14–16] and a zero-momentum bias satellite [17–19]. A number of papers are available describing different strategies and approaches examined and implemented where the controllers were basically designed based on the linear and non-linear control techniques.

In this paper, the algorithm for an optimum magnetic torque generation for controlling a momentum bias satellite is discussed. A bias momentum system takes advantage of the gyroscopic stiffness effect of a spinning object. It is implemented by placing a momentum wheel along the pitch axis [20]. The nominal angular momentum value provided by the wheel keeps this axis inertially fixed as well as stiffens the roll/yaw axes thus enabling the 3-axis stabilization. Although this technique provides the 3-axis stabilization, it is difficult to provide a high pointing accuracy along all the three axes as the momentum wheel induces the nutation effect and the wheel itself tends to get saturated [21]. Therefore, an additional actuator is necessary on this satellite to eliminate the nutation and unload the excessive

angular momentum of the wheel in order to achieve a high pointing accuracy along all the three axes. Magnetic technique has been a primary option in dealing with these issues because it is lightweight, requires low power consumption and inexpensive. Therefore, the algorithm structured herein is for controlling the satellite attitudes, nutation and momentum unloading of the wheel implementing two and three magnetic torquers onboard. This work is the extension of the previous work done by Mohd Suhadis and Varatharajoo [22].

2. THE GEOMAGNETIC FIELD

The existence of the geomagnetic field is believed to have been generated within the Earth. The theories about it are reviewed in details by Jacobs [23] and Campbell [24]. It can be concluded here that there are three main sources that contribute to this field. The main magnetic field B_m which accounts for over 95% of the total intensity comes from a self-excited dynamo effect of the Earth's core. This generated field consequently magnetized the crustal rocks in outer layer of the Earth thus generating another small amount of magnetic field B_c. Then, another small amount of magnetic field B_d arises from the electrical current flowing in the ionized upper atmosphere. These productions of the geomagnetic fields can be summarized in a mathematical equation as [25]

$$\mathbf{B}(\mathbf{r}, t) = \mathbf{B}_m(\mathbf{r}, t) + \mathbf{B}_c(\mathbf{r}) + \mathbf{B}_d(\mathbf{r}, t) \tag{1}$$

However, the contribution of the last two sources is very minimal and can be eliminated during the modeling process.

Since the existence of the geomagnetic field is practically arises from the motion of electrons, the mathematical model of the field derived is based on the Maxwell's equations. However, the assumption has been made that the amount of current flowing across the boundary between the Earth and its atmosphere is almost null and this implies that at the Earth surface the curl of the vector **B** is zero, thus the vector field can be written as the negative gradient of a potential function as follows [24]

$$\nabla \times \mathbf{B} = 0 \tag{2}$$

$$\mathbf{B} = -\nabla V \tag{3}$$

In this case, the divergence of magnetic dipole vector field is considered zero because the magnetic flux directed inward the south-pole is equal to the flux outward the north-pole.

$$\nabla \cdot \mathbf{B} = 0 \tag{4}$$

The combination of Eq. (3) and Eq. (4) satisfies the Laplace equation that can be written as

$$\nabla^2 V = 0 \tag{5}$$

Since the earth is approximately spherical, this Laplace equation can be solved in terms of spherical harmonics [26],

$$V\left(r,\theta,\lambda\right) = R\sum_{n=1}^{k}\left(\frac{R}{r}\right)^{n+1}\sum_{m=0}^{n}\left(g_n^m \cos m\lambda + h_n^m \sin m\lambda\right)P_n^m\left(\theta\right) \tag{6}$$

where R is the equatorial radius of the earth, (r, θ, λ) are the geocentric distance, co-latitude and east longitude from Greenwich, (g_n^m, h_n^m) are the Schmidt normalized Gaussian coefficients and $P_n^m(\theta)$ is the associated Legendre functions. The Schmidt normalized Gaussian coefficients are determined from sets of measured data obtained from the satellites and ground observatories scattered around the world by a least-squares fit technique. These coefficients are revised every 5 years because the geomagnetic field is constantly changing with time. Two main models of Gaussian coefficients that are available are the International Geomagnetic Reference Field (IGRF) and the World Magnetic Model (WMM) [25]. The former is from the International Association for Geomagnetism and Aeronomy (IAGA) and the latter is a product of the U.S National Oceanic and Atmospheric Administration (NOAA) in collaboration with the British Geological Survey (BGS). In this work, the IGRF model has been chosen. The general solution of this function expressed in spherical coordinate system can be written as follows

$$B_r = \frac{-\partial V}{\partial r} \tag{7a}$$

$$B_\theta = \frac{-1}{r}\frac{\partial V}{\partial \theta} \tag{7b}$$

$$B_\lambda = \frac{-1}{r\sin\theta}\frac{\partial V}{\partial \lambda} \tag{7c}$$

The geomagnetic field also can be written into a much simpler form with the assumption that the effects of Earth rotation and orbit precession are negligible for the duration of simulation. The simplified model of this field expressed in the Local Vertical Local Horizontal (LVLH) coordinate system is defined as follows [27]

$$\begin{bmatrix} B_x(t) \\ B_y(t) \\ B_z(t) \end{bmatrix}_{LVLH} = \begin{bmatrix} b_x \cos(\omega_0 t) \\ -b_y \\ b_z \sin(\omega_0 t) \end{bmatrix} \tag{8}$$

where the time t is measured from 0 at the ascending node of the orbit relative to the geomagnetic equator and b_x, b_y and b_z are constant values with the magnetic field's dipole strength μ_f equal to $7.9 \times 10^{15} Wb \cdot m^{-1}$

$$b_x = \left(\frac{\mu_f}{R_{orbit}^3}\right)\sin(i) \tag{9a}$$

$$b_y = \left(\frac{\mu_f}{R_{orbit}^3}\right)\cos(i) \tag{9b}$$

$$b_z = 2\left(\frac{\mu_f}{R_{orbit}^3}\right)\sin(i) \tag{9c}$$

Simulation has been carried out for both models with the orbital parameters described in Table 1. The values of the Complex Geomagnetic Field Model (CFGM) expressed in the local vertical local horizontal coordinate system have been plotted in Figure 1 while the values of the Simplified Geomagnetic Field Model (SFGM) have been plotted in Figure 2. In this paper, tuning of the control gains for the validation of the attitude control structure is based on the SGFM. Then, the same gains are used to simulate the control structure using the CGFM.

Table 1 Orbital parameters

Parameters	**Value**
Altitude, h	540 km
Inclination, i	53°
Eccentricity, e	≈ 0
Right ascension of ascending node, Ω	0°
Argument of perigee, ω	0°
True anomaly, v	0°
Simulation time, t	5 orbits
Epoch	1 April 2010
Orbital frequency, ω_0	0.0011 $rads^{-1}$

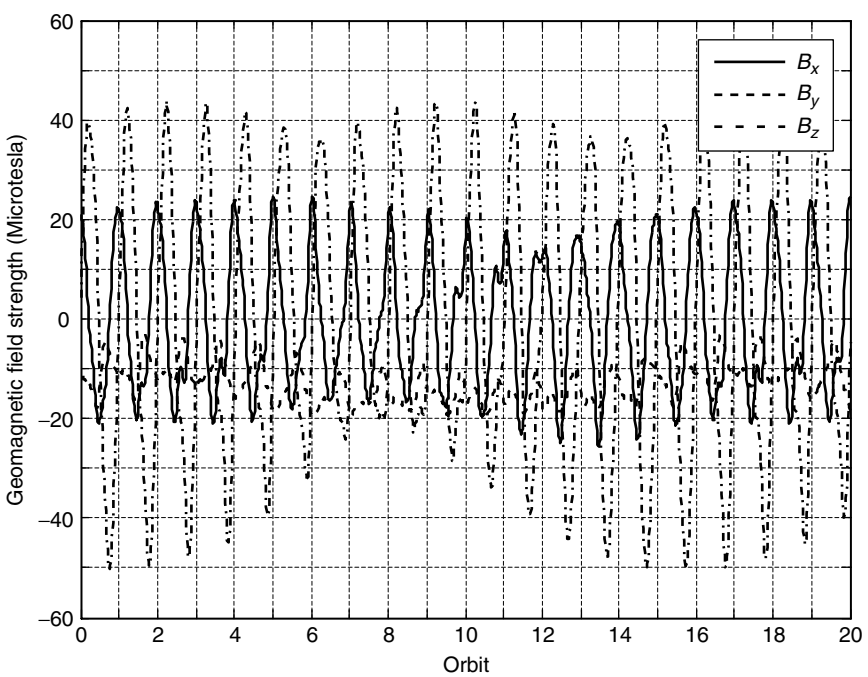

Figure 1 The CGFM along the specified orbit.

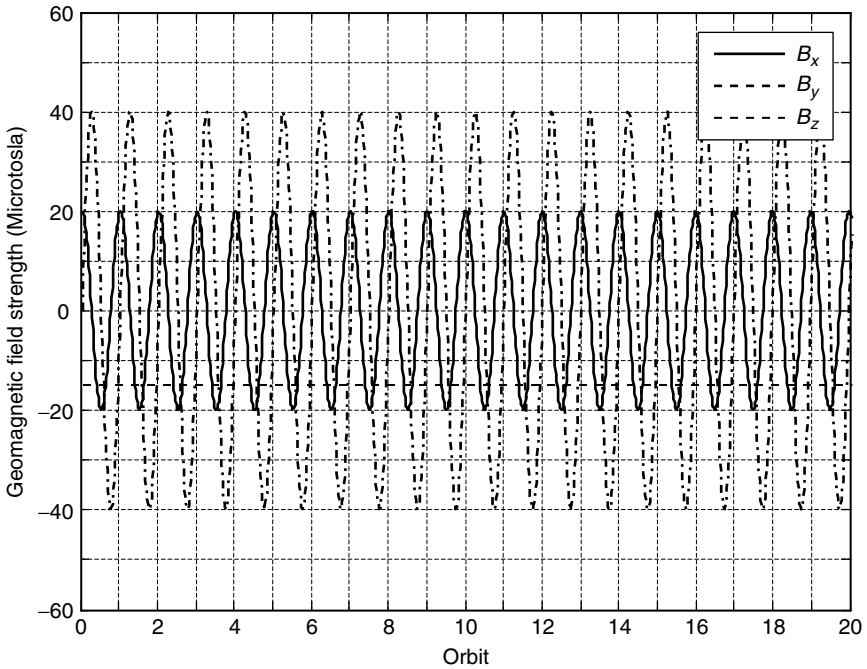

Figure 2 The SGFM along the specified orbit.

3. MAGNETIC TORQUE GENERATION

As stated previously, the magnetic control torque is produced when the magnetic dipole moment generated within the satellite couples with the geomagnetic field. This interaction can be mathematically described as follow

$$\mathbf{T}_m = \mathbf{M} \times \mathbf{B} \tag{10}$$

where $\mathbf{T}_m$ is the magnetic torque vector, $\mathbf{M}$ is the satellite's magnetic dipole moment vector generated by magnetic torque and $\mathbf{B}$ is the geomagnetic field vector. This equation clearly explains that the generation of magnetic torques is constrained to be perpendicular to both the satellite's magnetic dipole moment and the geomagnetic field.

3.1. MAGNETIC TORQUER

A magnetic torquer consists of a coil and a core as depicted in Figure 3 where the magnetic dipole moment is generated by a passing electrical current through the coil. There are two types of magnetic torquer used for satellite controls, i.e., the air core or the magnetic core. The magnetic core dramatically amplifies the produced magnetic field to several hundred times than that of the equivalent air core. The choice of the material used as magnetic core is very important as it will affect the amount of required power by the magnetic torquer as well as its total mass. The magnetic core with high relative permeability causes a decrease in the required power by the magnetic torquer and reduces its mass [28]. Ferromagnetic materials such as iron-cobalt or nickel-iron not only have a high level of permeability but magnetic torquer that uses this material as the magnetic core also has a linear relationship between the input current and the magnetic dipole moment within its specified linear range.

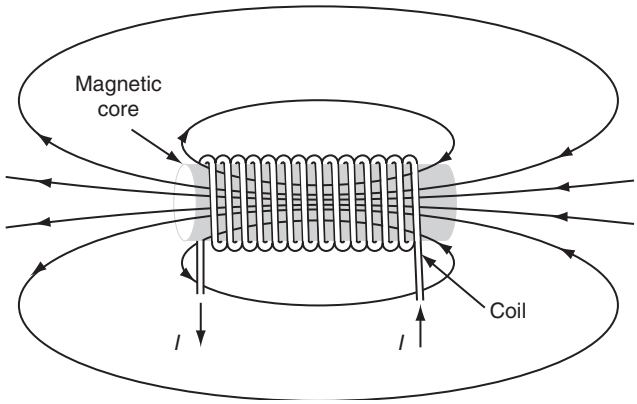

Figure 3 Schematic diagram of magnetic torque.

3.2. CONTROL ALGORITHM

The formulation of the control structures are based on the well known momentum unloading controller [20]

$$\mathbf{T} = -k\Delta\mathbf{h} \tag{11}$$

where k is the unloading control gain while $\Delta\mathbf{h}$ is the excess momentum. Inserting this equation into Eq. (10) yields

$$-\boldsymbol{k}\Delta\mathbf{h} = \mathbf{M} \times \mathbf{B} \tag{12}$$

However, the matrix **B** in Eq. (12) is singular thus it cannot be inverted to find the values of **M** needed to be generated by each magnetic torquer onboard the satellite. Arduini and Baiocco [29] explained that this problem can be solved by multiplying both sides of Eq. (12) with **B** and solving for **M** to get the equation that represents the optimum value of the satellite's magnetic dipole moment needed to be generated by each magnetic torquer.

$$\mathbf{M} = -\frac{\mathbf{k}}{B^2}\left(\mathbf{B} \times \Delta\mathbf{h}\right) \tag{13}$$

Then, the total magnetic control torque can be defined by inserting Eq. (13) into Eq. (10)

$$\mathbf{T}_m = -\frac{\mathbf{k}}{B^2}\left(\mathbf{B} \times \Delta\mathbf{h}\right) \times \mathbf{B} \tag{14}$$

4. SATELLITE CONFIGURATION

Two satellite models are configured as depicted in Figure 4. Each of these satellites is equipped with 2 and 3 magnetic torquers that are strategically used for controlling the satellite attitudes, nutation and momentum unloading of the wheel. The dynamic equation of this satellite is defined as follow

$$\left(\dot{\mathbf{h}}_s + \dot{\mathbf{h}}_w\right) + \boldsymbol{\omega} \times \left(\mathbf{h}_s + \mathbf{h}_w\right) = \mathbf{T} \tag{15}$$

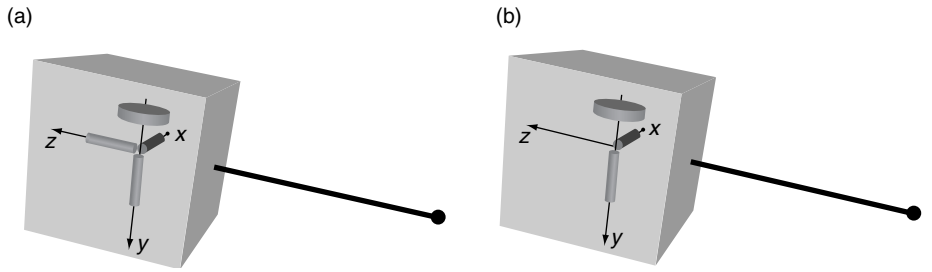

Figure 4 Momentum bias satellite with (a) 3 magnetic torquers and (b) 2 magnetic torquers.

The external torques, $\mathbf{T} = [T_x\ T_y\ T_z]^T$ consists of two essential parts which are the disturbance torque, $\mathbf{T}_d = [T_{dx}\ T_{dy}\ T_{dz}]^T$ and the control torque, $\mathbf{T}_c = [T_{cx}\ T_{cy}\ T_{cz}]^T$. Their relation can be defined as follows

$$\mathbf{T} = \mathbf{T}_d + \mathbf{T}_c \tag{16}$$

In this work, the disturbance torque consists of the gravity gradient, aerodynamic, magnetic and solar radiation torques, while the control torque is generated by the onboard magnetic torquers.

After linearization, the dynamic equations of the satellite along roll and yaw axes defined for the attitude and nutation are as follow [30, 31]

$$\begin{bmatrix} \dot{h}_{0x} \\ \dot{h}_{0z} \end{bmatrix} = \begin{bmatrix} 0 & \omega_0 \\ -\omega_0 & 0 \end{bmatrix} \begin{bmatrix} h_{0x} \\ h_{0z} \end{bmatrix} + \begin{bmatrix} 1 & 0 \\ 0 & 1 \end{bmatrix} \tag{17}$$

$$\begin{bmatrix} \dot{\omega}_x \\ \dot{\omega}_z \end{bmatrix} = \begin{bmatrix} 0 & -h_{wy}/I_x \\ h_{wy}/I_x & 0 \end{bmatrix} \begin{bmatrix} \omega_x \\ \omega_z \end{bmatrix} + \begin{bmatrix} 1/I_x & 0 \\ 0 & 1/I_z \end{bmatrix} \begin{bmatrix} T_x \\ T_z \end{bmatrix} \tag{18}$$

Since the momentum wheel gives the perfect attitude pointing along the pitch axis [32], only the task of controlling the angular momentum value of the wheel is of interest herein. Thus, linearized equation along the pitch axis only considering the angular momentum of the wheel which is written as follows

$$\begin{bmatrix} \dot{h}_{wy} \end{bmatrix} = \begin{bmatrix} 1 \end{bmatrix} \begin{bmatrix} T_y \end{bmatrix} \tag{19}$$

General control principle used for both of these satellites is as follows

$$\mathbf{T}_m = \mathbf{T}_{Attitude\ /\ wheel\ momentum} + \mathbf{T}_{Nutation} \tag{20}$$

where for the total magnetic control torque from the attitude and momentum wheel contribution $\Delta \boldsymbol{h} = [h_{0x}\ \Delta h_w\ h_{0z}]^T$ while for the nutation contribution $\Delta \boldsymbol{h} = [\omega_x\ \omega_z]^T$.

Each magnetic torquer in these satellites is assigned with different tasks. With regard to that, the control strategies of these satellites are developed and described in Table 2. Based on Eq. (13), the amount of magnetic dipole moment need to be generated by each magnetic torquer onboard both satellites are defined by equations described in Tables 3 and 4.

Table 2 Control strategy

Satellite	**Magnetic torquers**	**Task (to control)**
With 3 magnetic torquers	Along x -axis	Momentum unloading
	Along y -axis	Roll/Yaw attitude and nutation
	Along z -axis	Momentum unloading
With 2 magnetic torquers	Along x -axis	Momentum unloading
	Along y -axis	Roll/Yaw attitude and nutation

Table 3 Control law for satellite with 3 magnetic torquers

Attitude, control	$M_{By} = \frac{\left(B_y B_{A31} - B_z B_{A21}\right)}{B^2} h_{0x} + \frac{\left(B_x B_{A23} - B_y B_{A13}\right)}{B^2} h_{0z}$
Nutation control	$M_{By} = -\frac{B_z B_{N21}}{B^2}\omega_x + \frac{B_x B_{N22}}{B^2}\omega_z$
Momentum unloading	$M_{Bx} = \frac{B_z B_{A12}}{B^2}\left(\frac{k_{P_{Bx}} \cdot s + 1}{s}\right)\Delta h_w$
	$M_{Bz} = -\frac{B_x B_{A32}}{B^2}\left(\frac{k_{P_{Bz}} \cdot s + 1}{s}\right)\Delta h_w$

Table 4 Control law for satellite with 2 magnetic torquers

Attitude control	$M_{cy} = -\frac{B_z C_{A21}}{B^2} h_{0x}$ $M_{cx} = -\frac{B_y C_{A13}}{B^2} h_{0z}$
Nutation control	$M_{cy} = -\frac{B_z C_{N21}}{B^2}\omega_x + \frac{B_x C_{N22}}{B^2}\omega_z$
Momentum unloading	$M_{cx} = \frac{B_z C_{A12}}{B^2}\left(\frac{k_{P_{cx}} \cdot s + 1}{s}\right)\Delta h_w$

5. NUMERICAL TREATMENTS

Series of simulations have been performed in order to verify the developed algorithm for each of configured satellites. Simulations are performed using the MATLAB® SIMULINK® software. Details of the satellite parameters and control parameters are given in Tables 5 and 6, respectively.

5.1. 3-MAGNETIC TORQUERS

The roll and yaw attitude performances of this satellite option are depicted in Figure 5. The plots show that these axes achieve the steady state attitude error after an orbit where the roll axis oscillates with and accuracy between –0.05˚ and 0.15˚ while the yaw axis oscillates between –0.05˚ and 0.3˚ with the SGFM. Meanwhile, the performance with the CGFM is not constant throughout the orbit with overall accuracy between –0.2˚ and 0.2˚ along the roll axis while between –0.2˚ and –0.4˚ along the yaw axis. This variation is actually reflection of the geomagnetic field values throughout the orbit where the oscillation is small when the geomagnetic field values are at maximum and vice versa.

Table 5 Satellite parameters

Parameter	Value
Weight	50 kg
Dimension	$690 \times 366 \times 366$ mm
I_x	178 kgm^2
I_y	181 kgm^2
I_z	4.3 kgm^2
h_{wy}	8.04 Nms
^{M}*magnetic torquer*	15 Am^2
Input	$T_{dx} = 12.8 \times 10^{-6} + 8.6 \times 10^{-6} \sin(\omega_0 t)$ Nm
	$T_{dy} = 55 \times 10^{-6} + 55 \times 10^{-6} \sin(\omega_0 t)$ Nm
	$T_{dz} = 12.8 \times 10^{-6} + 4.3 \times 10^{-6} \sin(\omega_0 t)$ Nm
Initial conditions	$\phi(0) = 5^\circ$, $\theta(0) = 5^\circ$, $\psi(0) = 5^\circ$
	$\omega_x(0) = 0$, $\omega_z(0) = 0$

Table 6 Control parameters

Satellite	With 3 magnetic	With 2 magnetic torquers
Attitude, gains	$B_{A13} = 0$	
	$B_{A21} = -0.002$	$C_{A13} = -0.002$
	$B_{A23} = 0.002$	$C_{A21} = -0.002$
	$B_{A31} = 0$	
Nutation gains	$B_{N21} = -1.2$	$C_{N21} = -1.2$
	$B_{N22} = 1.2$	$C_{N22} = 1.2$
Momentum unloading gains	$B_{A12} = B_{A32} = k_{I_B}$	$C_{A12} = k_{I_C}$
	$k_{I_B} = \omega_n^2$	$k_{I_C} = \omega_n^2$
	$k_{P_{Bx}} = k_{P_{Bz}} = \frac{2\xi}{\omega_n}$	$k_{P_{Cx}} = \frac{2\xi}{\omega_n}$
	$\omega_n = 4 \times 10^{-3}$	$\omega_n = 4 \times 10^{-3}$
	$\xi = 1$	$\xi = 1$

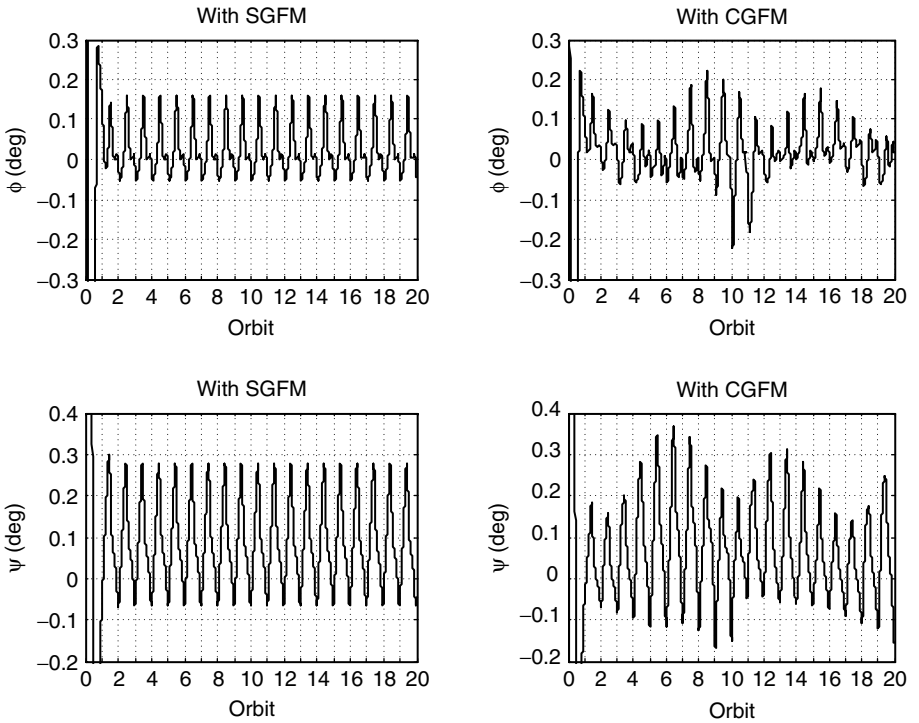

Figure 5 The attitude performance of the satellite with 3 magnetic torquers.

The total value of magnetic dipole moments generated by each magnetic torquer onboard the satellite is shown in Figure 6. It can be seen that the generated values are almost similar with both the SGFM and CGFM where between $-1\ Am^2$ and $3\ Am^2$ along the roll axis, between $0\ Am^2$ and $2\ Am^2$ along the pitch axis and within $\pm 3\ Am^2$ along the pitch axis. Whereas the total magnetic torque generated when the magnetic torquers onboard the satellite couple with the geomagnetic field is depicted in Figure 7. Again the generated magnetic torque in each axis almost similar with both the SGFM and CGFM where within $\pm 5 \times 10^{-5} Nm$ is generated along the roll axis, between 0 and $-10 \times 10^{-5} Nm$ along the pitch axis and within $\pm 5 \times 10^{-5} Nm$ along the yaw axis.

5.2. 2-MAGNETIC TORQUERS

The attitude performance along the roll and yaw axes is shown in Figure 8 where both axes take about two orbits to reach their steady state attitude values which are a bit longer compared to the satellite with 3 magnetic torquers. As for the SGFM, the roll axis oscillates with accuracy within $\pm 0.5^\circ$ and the yaw axis oscillates between -0.7° and 0.6°. While for the CGFM, the overall accuracy is within $\pm 0.5^\circ$ along the roll axis and between -1° and 0.6° along the yaw axis.

Figure 9 shows the total value of magnetic dipole moments generated by each magnetic torquer onboard the satellite. The magnetic torquer along the roll axis generates between $-10\ Am^2$ and $5\ Am^2$ while the magnetic torquer along the pitch axis generates within $\pm 1\ Am^2$ for the SGFM. While for the CGFM, the maximum value of magnetic dipole moments generated by the magnetic torquer throughout the orbit along the roll axis is between $-15\ Am^2$ and $6\ Am^2$ and between $-4\ Am^2$ and $6\ Am^2$ along the pitch axis.

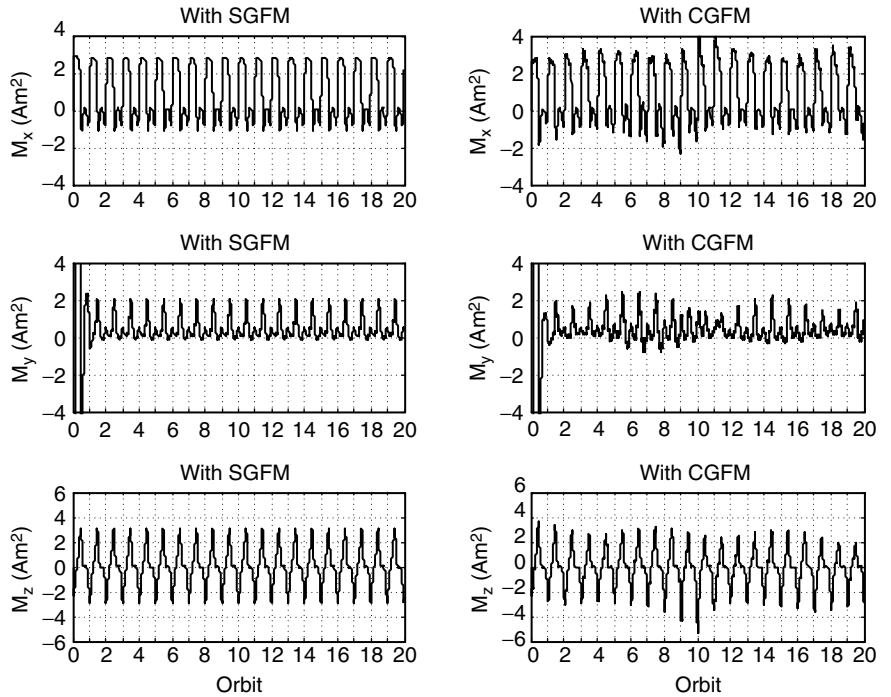

Figure 6 The magnetic dipole moment generated by magnetic torquers onboard the satellite with 3 magnetic torquers.

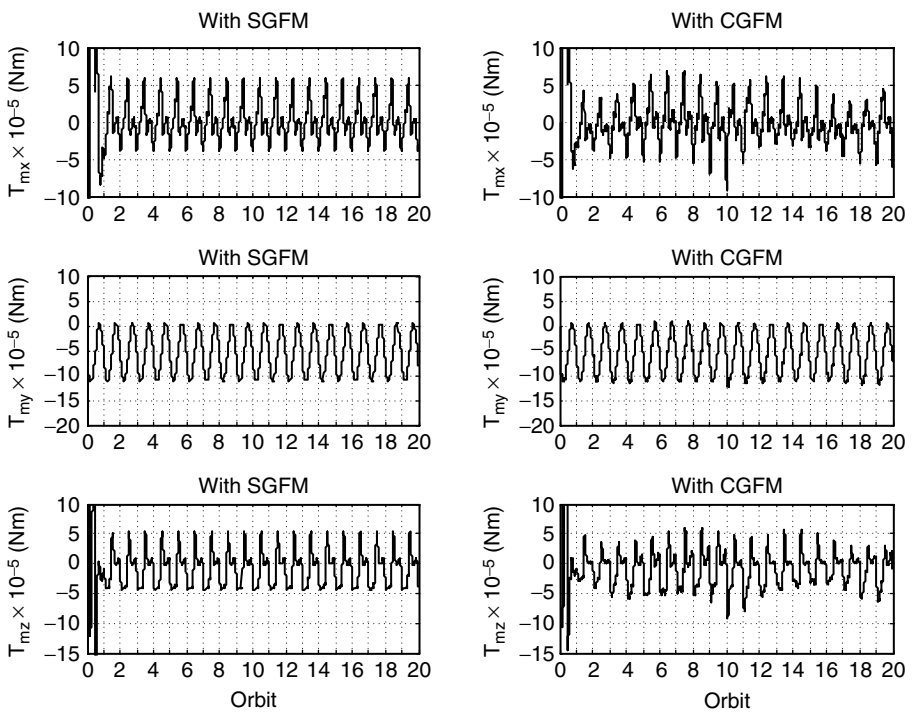

Figure 7 The magnetic torque generated onboard the momentum bias satellite with 3 magnetic torquers.

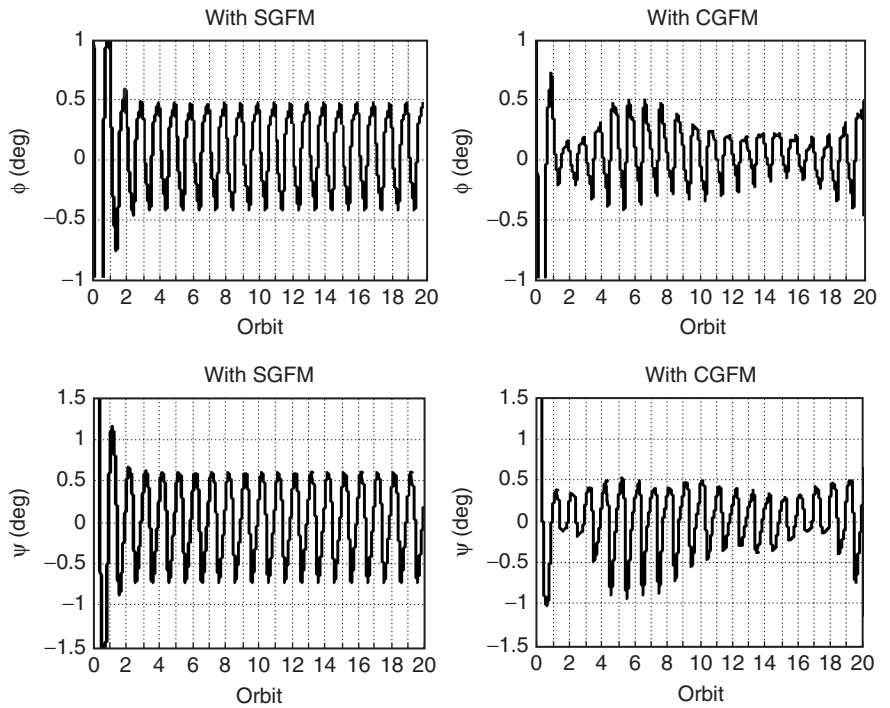

Figure 8 The attitude performance of the satellite with 2 magnetic torquers.

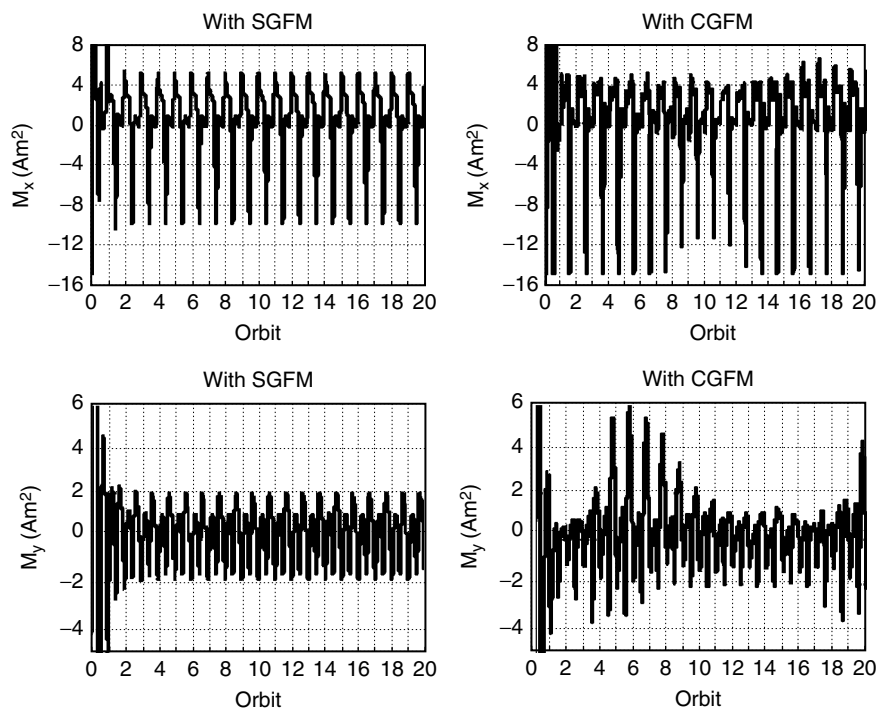

Figure 9 The magnetic dipole moment generated by magnetic torquers onboard the satellite with 2 magnetic torquers.

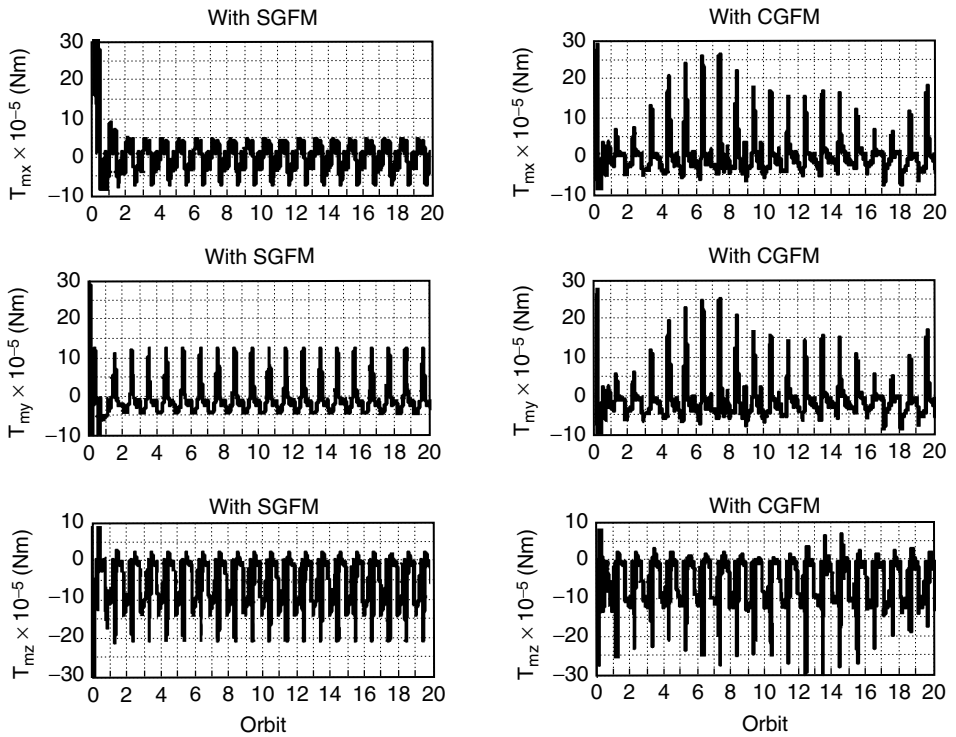

Figure 10 The magnetic torque generated onboard the momentum bias satellite with 2 magnetic torquers.

The total magnetic torque generated along the satellite's primary axes is depicted in Figure 10. It can be seen that with SGFM, the total generated torque is between 5×10^{-5} *Nm* and -10×10^{-5} *Nm* along the roll axis, between 15×10^{-5} *Nm* and -5×10^{-5} *Nm* along the pitch axis and between 2.5×10^{-5} *Nm* and -20×10^{-5} *Nm* along the yaw axis. While with CGFM, the maximum total generated torque throughout the orbit is between 25×10^{-5} *Nm* and -5×10^{-5} *Nm* along the roll axis, between 25×10^{-5} *Nm* and -10×10^{-5} *Nm* along the pitch axis and between 5×10^{-5}*Nm* and -30×10^{-5} *Nm* along the yaw axis.

6. CONCLUSION

In this paper, the attitude torque generation of the momentum bias satellite employing 2 and 3 magnetic torquers onboard has been studied. Two algorithms for an optimum magnetic torque generation for controlling a momentum bias satellite based on 2 or 3 magnetic torquers have been discussed. For validation purposes, both algorithms have been tested with the SGFM and CGFM. Numerical treatments were performed using the MATLAB® SIMULINK® codes. Results from the simulations show that the attitude performance of both satellite configurations fulfills the satellite mission requirements. However, the satellite that uses 3 magnetic torquers onboard provides a better torque generation compartment compared to the satellite that only uses 2 magnetic torquers onboard which gives a better attitude performance.

ACKNOWLEDGEMENT

The work presented in this paper has been supported by the Universiti Sains Malaysia Short Term Research Grant Scheme.

REFERENCES

[1] S.K. Shrivastava and V.J. Modi, Satellite attitude dynamics and control in the presence of environmental torques – A brief survey, *Journal of Guidance, Control and Dynamics*, 1983, 6(6), 461–471.

[2] F. Mesch, Magnetic components for the attitude control of space vehicles. *IEEE Transaction of Magnetics*, 1969, 5(3).

[3] R. E. Fischell, Passive magnetic attitude control for earth satellites. *Advances in the Astronautical Sciences*, 1962, Vol. 11, 147–176.

[4] B. M. Menges and C. A. Guadiamos, Dynamic modeling of micro-satellite SPARTNIK's attitude, *36th Aerospace Sciences Meeting and Exhibit*, January 12–15, 1997.

[5] M. Ovchinnikov and V. Pen'kov, Attitude control system for the first sweedish nanosatellite "MUNIN". *Acta Astronautica*, 1999, 46(2–6), 319–326.

[6] F. Santoni and M. Zelli, Passive magnetic attitude stabilization of the UNISAT-4 microsatellite. *Acta Astronautica*, 2009, 65(5–6), 792–803.

[7] J.S. White, F.H. Shigemoto, and K. Bourquin, Satellite attitude control utilizing the Earth's magnetic field. *Technical Report NASA TN-D1068, National Aeronautics and Space Administration*, 1961.

[8] E. I. Ergin, and P. C. Wheeler, Magnetic attitude control of a spinning satellite. *Journal of Spacecraft and Rockets*, 1965, 2(6), 846–850.

[9] P.C. Wheeler, Spinning spacecraft attitude control via the environmental magnetic field. *Journal of Spacecraft and Rockets*, 1967, 4(12), 1631–1637.

[10] P. Rozenfeld, V. Orlando, and R.R.B. Miguez, SCD1 three years in orbit operation. *4th International Symposium on Space Mission Operations and Ground Data System-SPACEOPS-96*, Munchen, Germany, 1996.

[11] I.M. Fonseca, P.N Souza, J.C.A.F Neri, and U.T.V. Guedes, The Attitude Control Subsystem of the Brazilian Scientific Satellite - SACI-1. *ICONE'96 Second International Conference on Non-Linear Dynamics, Chaos, Control and Their Applications in Engineering Sciences*, São Pedro, SP, Brazil, 1996.

[12] T. Bak, M. Blanke, and R. Wisniewski, Flight results and lessons learned from the ørsted attitude control systems. *4th ESA International Conference*, Noordwijk, the Netherlands, 2000.

[13] J. Miau, and J. Juang, LEAP: A Student Microsatellite Design Project. *International Conference on Engineering Education & Research*, Melbourne, Australia, 2007.

[14] T. Mizuno, H. Saito, Y. Masumoto, T. Oshima, M. Hashimoto, A. Choki, A. Miura, H. Ogawa, S. Tachikawa, K. Tanaka, Y. Kuroda, and I. Nakatani, INDEX: A piggy-back satellite for advanced technology demonstration. *13th Annual AIAA/USU Conference on Small Satellites*, 1999.

[15] Y. Zheng, G. Ke, M. Sweeting, Tsinghua micro/nanosatellite research and it's application. *13th Annual AIAA/USU Conference on Small Satellites*, 1999.

[16] N. Hamzah, and Y. Hashida, TiungSAT-1 momentum wheel commissioning. *World Engineering Congress*, Kuala Lumpur, 2001.

[17] B.J. Kim, H. Lee, and S.D. Choi, Three-axis reaction wheel attitude control system for KITSAT-3 microsatellites, *IFAC Conference on Autonomous and Intelligent Control in Aerospace*, Beijing, China, 1995.

[18] Z. Sun, Y. Cheng, Y. Geng, and X. Cao, The active magnetic control algorithm for HITSAT-1. *Aircraft Engineering and Aerospace Technology: An International Journal*, 2000, 72(2), 137–141.

[19] A. Skullestad, and J.M. Gilbert, H_{∞} control of a gravity gradient stabilized satellite. *Control Engineering Practice*, 2000, 8(9), 975–983.

[20] M.J. Sidi, Spacecraft dynamics and control. *Cambridge University Press*, 1997.

[21] K. Tsuchiya, M. Inoue, N. Wakasuqi, and T. Yamaguchi, Advanced reaction control wheel controller for attitude control of spacecraft. *Acta Astronautica*, 1982, 9(12), 697–702.

[22] N. Mohd Suhadis, R. Varatharajoo, Satellite Attitude Performance during the Momentum dumping Mode, *International Review of Aerospace Engineering*, 2009, Vol. 3(2), pp. 133–138.

[23] J. A. Jacobs, Reversals of the earth's magnetic field (2nd ed.). *Cambridge University Press*, 1994.

[24] W.H. Campbell, Introduction to geomagnetic fields (2nd ed.). *Cambridge University Press*, 2003.

[25] S. McLean, S. Mcmillan, S. Maus, V. Lesur, A. Thompson, and D. Dater, The US/UK World Magnetic Model for 2005-2010. *NOAA Technical Report NESDIS/NGDC-1*, 2004.

[26] J.R. Wertz, Spacecraft attitude determination and control. *Kluwer Academic Publishers*, 1978.

[27] M. L. Psiaki, Magnetic torquer attitude control via asymptotic periodic linear quadratic regulation. *Journal of Guidance Control and Dynamics*, 2001, 24(2), 386–394.

[28] M.F. Mehrjardi, and M. Mirshams, Design and manufacturing of a research magnetic torquer rod. *Contemporary Engineering Sciences*, 2010, 3(5), 227–236.

[29] C. *Arduini*, C. and P. Baiocco, P. Active magnetic damping attitude control for gravity gradient stabilized spacecraft. *Journal of Guidance and Control*, 1997, 20(10), pp. 117–122.

[30] N. Mohd Suhadis, R. Varatharajoo, New Satellite Control Structure Using the Geomagnetic Field, *International Journal of Engineering and Technology*, 2006, Vol. 3(2), pp. 175–181.

[31] J. Bals, W. Fichter, and M. Surauer, Optimization of magnetic attitude and angular momentum control for low earth orbit satellites. *Proceedings Third International Conference on Spacecraft Guidance, Navigation and Control Systems*, ESTEC, Noordwijk, The Netherlands, 1996.

[32] R. Varatharajoo, and S. Fasoulas, The combined energy and attitude control system for small satellites – Earth observation mission. *Acta Astronautica*, 2005, 56(1–2), 251–259.